Title

The virtual axle concept for detection of localised damage using bridge weigh-in-motion data

Authors

Daniel Cantero[a,b], Raid Karoumi[a], Arturo González[c]

Affiliations

[a] Civil and Architectural Engineering, Royal Institute of Technology KTH, Stockholm, Sweden

[b] Roughan & O'Donovan Innovative Solutions, Arena Road, Arena House, Dublin 18, Ireland

[c] School of Civil, Structural and Environmental Engineering, University College Dublin, Dublin, Ireland

Emails:

Daniel Cantero: canterolauer@gmail.com

Raid Karoumi: raid.karoumi@byv.kth.se

Arturo González: arturo.gonzalez@ucd.ie

Corresponding Author full address

Daniel Cantero

e-mail: canterolauer@gmail.com

Telephone: 0046 8 790 7957

Postal Address: Brinellvägen 23, 10044 Stockholm, Sweden

Symbols

A_i = Weight of axle *i*

$\tilde{A}_i$ = Actual weight of axle *i*

B-WIM = Bridge WIM

C = Constant value

COV = Coefficient of variation

D = Auxiliary matrix

$D_{p,q}$ = Auxiliary matrix element

FEM = Finite Element Model

GVW = Gross Vehicle Weight

H = Auxiliary matrix

$H_{p,q}$ = Auxiliary matrix element

I = Vehicle's body moment of inertia

$I_{t,i}$ = Influence line value at sampling point *t* and axle *i*

$\tilde{I}_{t,i}$ = Current influence line value at sampling point *t* and axle *i*

L = Bridge span or length of influence line

N = Total number of vehicle axles

NOR = Nothing-On-Road

SHM = Structural Health Monitoring

SNR = Signal to Noise Ratio

T = Total number of sampling points

VA = Virtual Axle

VA^* = Virtual Axle indicator

VA_B = Back Virtual Axle

VA_F = Front Virtual Axle

WIM = Weigh-In-Motion

c_s = Vehicle's suspension damping

c_t = Vehicle's type viscous damping

d = axle distance

d_{VA} = Virtual Axle distance

k = damage indicator

k_H = damage indicator for healthy state

k_s = Vehicle's suspension stiffness

k_t = Vehicle's tyre stiffness

m = Vehicle's body mass

m_t = Vehicle's tyre mass

v = Vehicle's velocity

δ = Tolerance in WIM classification

ε_t = Strain at sampling point t

ε_t^{me} = Measured strain at sampling point t

ε_t^{th} = Theoretical strain at sampling point t

σ = standard deviation

Ψ = Objective function

1. Introduction

In any road or railway network the maintenance of bridges is a fundamental part of the infrastructure management. The main problems that the network owners face are the aging of these bridges and the inherent difficulty of performing accurate structural assessments without disrupting the traffic. There is a need for a cost effective and reliable assessment procedure. Many Structural Health Monitoring (SHM) techniques have been devised over the past decades. However, there is no particular solution that can be applied to all bridges and conditions. The authors believe that any reliable SHM system for bridges will be made of a combination of different techniques applicable to the financial constraints and particularities of the structure under consideration. Therefore, there is scope for new techniques complementing existing methods. This paper proposes a new level I damage identification method for short span statically indeterminate bridges using the information provided by a Bridge Weigh-in-Motion (B-WIM) system.

Weigh-In-Motion (WIM) systems comprehend a wide range of technologies that allow estimating wheel weights and axle distances of traversing vehicles moving at normal operational speed. In particular, Bridge-based WIM systems (B-WIM) use the structure's response to estimate the vehicle's load distribution. Generally, strain gauges record the deformation of the bridge while the vehicle of interest is traversing the structure. The original idea, first introduced by Moses in 1979 [1], is based on the concept of influence line which can be obtained on-site using a vehicle of known speed, axle distance and weights [2]. The algorithm searches for the load distribution that best fits the recorded response by minimizing the error with respect to an assumed

theoretical response. In modern B-WIM installations, it is common practice to use multiple locations of strain gauges along the span, which allow for axle counting and the accurate estimation of the distances between axles, an approach called Nothing-On-the-Road [3]. B-WIM is mostly used on road bridges, but it has been successfully used for railway traffic [4].

The use of B-WIM systems for SHM has only rarely been investigated in literature, and to the best of the authors' knowledge there are only few precedents. For instance, in [5] it is proposed to use the combined information of two independent WIM systems, one pavement-based and one bridge-based. Damage can then be detected by studying the ratio between weight estimates of both systems. On the other hand, in [6] a B-WIM installation is used as the input for an artificial neural network based algorithm. After sufficient learning process, this system is then able to predict a bridge response, which can be compared to the measurements. High predictions errors indicate that damage has occurred.

This paper suggests that B-WIM systems can be used for SHM simply by performing additional calculations on the measurements. It is theoretically shown that for a given vehicle it is convenient to assume the presence of an additional weightless axle, which has been termed 'Virtual Axle' (VA), to detect damage. A change in structural behaviour will lead to weight estimates different than zero for this fictitious VA load by the B-WIM system. It is possible to identify even small changes in influence line by applying the VA concept. The proposed idea, illustrated in Figure 1, can be used to define a new robust output-only model-free level 1 SHM technique. The VA concept can also be extended it to self-calibration of B-WIM systems.

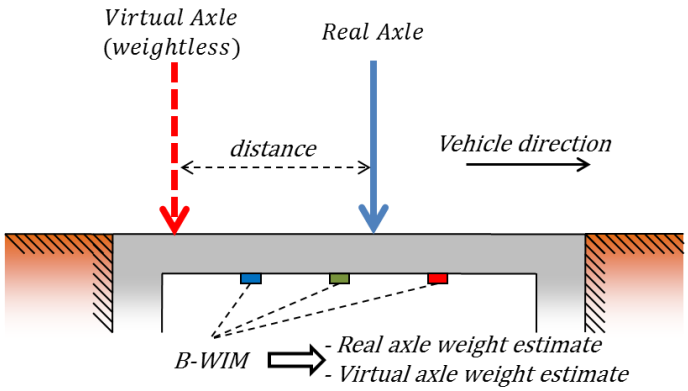

Figure 1: Schematic description of Virtual Axle idea

The VA concept is applicable to standard B-WIM systems that are already installed since no changes in hardware are required. It is only necessary to update the software to include the calculations of a fictitious load. However, its scope is limited to identification of local damages in statically indeterminate structures.

The content of the paper has been divided into two distinct parts, theoretical derivation and numerical validation. First, the theoretical study presents the theory behind the new concept and why it can be used for damage identification as well as its inherent limitations. The numerical validation of the VA idea starts by describing the vehicle-bridge interaction (VBI) models used for testing. Then the VA analysis is applied on two specific scenarios in order to define a correct damage indicator. Next, the VA concept is numerically tested using simulated results within a Monte Carlo framework and its performance compared to another level I SHM technique (changes in fundamental frequency). The influence of the key factors is studied separately for different degrees and locations of damage, noise levels, span lengths and profile irregularities. The paper ends with a discussion section that elaborates on the applicability of the method followed by conclusions.

2. Theoretical derivation

This section presents the theoretical explanation of why a VA in B-WIM systems provides additional information on the structure's behaviour. The axle weights of an N-axle vehicle are given by the vector in Eq. (1),

$$\{A_i\} = \{A_1 \quad A_2 \quad \cdots \quad A_N\}^T \qquad \text{Eq. (1)}$$

Then, the static strain defined at discrete time samples *t* and at any particular section of the structure due to the passing vehicle can be calculated using the influence line as in:

$$\{\varepsilon_t\} = [I_{t,i}]\{A_i\} \qquad \text{Eq. (2)}$$

where $\{\varepsilon_t\}$ is the strain vector of dimension $(T \times 1)$ and $[I_{t,i}]$ is the matrix of influence line's ordinates of dimension $(T \times N)$. T is the total number of sampling points. The matrix $[I_{t,i}]$ is composed of multiple copies of the influence $\{I_t\}$ line for the particular sensor location considered and shifted accordingly to the axle spacings of the vehicle. Figure 2 shows an example of the values of the influence line matrix for the case of a 2-axle vehicle over a fixed-fixed beam, where each line shows the individual contribution of each unit axle to the total static strain.

The B-WIM algorithm [1] searches for the axle weights that best fits the recorded response by minimizing the error with an assumed theoretical response. The objective

function to be minimised, in the least squares analysis, is the difference between measured ε_t^{me} and theoretical strain ε_t^{th}:

$$\Psi = \sum_{t=1}^{T} \left(\varepsilon_t^{me} - \varepsilon_t^{th}\right)^2 \qquad \text{Eq. (3)}$$

Using Eq. (2) for the theoretical strain and expanding the expression gives:

$$\Psi = \{A_i\}^T \left[I_{t,i}\right]^T \left[I_{t,i}\right]\{A_i\} - 2\{A_i\}\left[I_{t,i}\right]\{\varepsilon_t^{me}\} + \{\varepsilon_t^{me}\}^T\{\varepsilon_t^{me}\} \qquad \text{Eq. (4)}$$

The minimum is the solution of Eq. (5), which is the first derivative of the objective function with respect to the vector of axle weights.

$$\frac{d\Psi}{d\{A_i\}} = 2\left(\left[I_{t,i}\right]^T\left[I_{t,i}\right]\right)\{A_i\} - 2\left[I_{t,i}\right]\{\varepsilon_t^{me}\} = 0 \qquad \text{Eq. (5)}$$

Solving Eq. (5) for the axle weights gives:

$$\{A_i\} = \frac{\left[I_{t,i}\right]^T\{\varepsilon_t^{me}\}}{\left[I_{t,i}\right]^T\left[I_{t,i}\right]} \qquad \text{Eq. (6)}$$

This result is the basic equation of the B-WIM algorithm expressed in matrix form. Further details on its derivation can be found in [7] and [8].

When a B-WIM system is installed for the first time it needs to be calibrated. The most important result during the calibration process is the structure's influence line $\{I_t\}$. This

is generally obtained using vehicles with known axle weights and axle spacings. Once calibrated, it is then possible to calculate the axle weights of any vehicle that traverses the bridge by recording the strain and solving the linear system in Eq. (6).

Over time the influence line might change because of structural damage or environmental conditions. We define the current influence line as $\{\tilde{I}_t\}$ which might be different to the one obtained during calibration. Based on Eq. (2), the measured strain can be approximated now as:

$$\{\varepsilon_t^{me}\} \approx \left[\tilde{I}_{t,i}\right]\{\tilde{A}_i\} \qquad \text{Eq. (7)}$$

where $\tilde{A}_i$ are the axle loads currently traversing the bridge. However, the installed B-WIM system continues estimating the axle weights with the information obtained during calibration. This can be mathematically expressed substituting Eq. (7) into Eq. (6) and gives:

$$\{A_i\} = \frac{\left[I_{t,i}\right]^T\left[\tilde{I}_{t,i}\right]\{\tilde{A}_i\}}{\left[I_{t,i}\right]^T\left[I_{t,i}\right]} \qquad \text{Eq. (8)}$$

It is possible to arrive to the analytical expression of the solution of Eq. (8). In particular, this has been derived for the case of a vehicle with two axles (N=2) separated by a distance d. Figure 2 shows the columns values of the current $\left[\tilde{I}_{t,i}\right]$ and at calibration $\left[I_{t,i}\right]$ influence line matrices for a fixed-fixed beam of length L affected by an unrealistic local stiffness reduction of 75% near mid-span. This huge damage was included in order to be able to visually discern the healthy from the damaged influence lines in Figure 2.

However, note that the degree of stiffness reductions considered in subsequent sections reaches only values up to 30%.

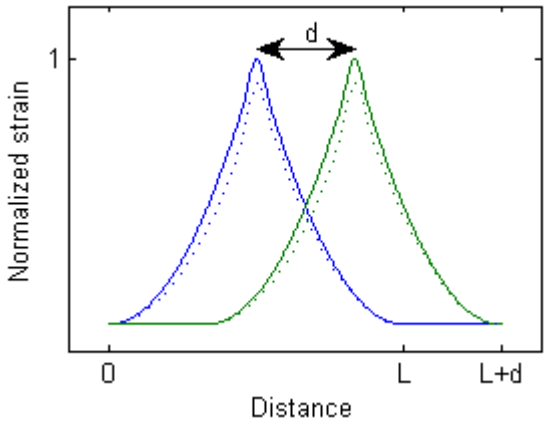

Figure 2: Influence lines of strain at mid-span shifted by an axle distance *d*. Solid lines = Healthy bridge. Dashed lines = Unrealistic damage near mid-span of 75% stiffness reduction with a length of 5% of *L*.

The matrix products in Eq. (8) can be rewritten for the 2-axle vehicle case as in Eq. (9) and Eq. (10), and simplified using the notation presented in Eq. (11) and Eq. (12). For clarity, the notation has been given the names *H* for the product of healthy influence lines and *D* for the damaged case (product of one healthy and one damaged influence line).

$$[I_{t,i}]^T[I_{t,i}] = \begin{bmatrix} \sum_{t=1}^{T} I_{t,1}^2 & \sum_{t=1}^{T} I_{t,1}I_{t,2} \\ \sum_{t=1}^{T} I_{t,2}I_{t,1} & \sum_{t=1}^{T} I_{t,2}^2 \end{bmatrix} = \begin{bmatrix} H_{1,1} & H_{1,2} \\ H_{2,1} & H_{2,2} \end{bmatrix} \quad \text{Eq. (9)}$$

$$\left[I_{t,i}\right]^T\left[\tilde{I}_{t,i}\right]=\begin{bmatrix}\sum_{t=1}^{T} I_{t,1}\tilde{I}_{t,1} & \sum_{t=1}^{T} I_{t,1}\tilde{I}_{t,2}\\ \sum_{t=1}^{T} I_{t,2}\tilde{I}_{t,1} & \sum_{t=1}^{T} I_{t,2}\tilde{I}_{t,2}\end{bmatrix}=\begin{bmatrix}D_{1,1} & D_{1,2}\\ D_{2,1} & D_{2,2}\end{bmatrix} \quad \text{Eq. (10)}$$

$$H_{p,q}=\sum_{t=1}^{T} I_{t,p}I_{t,q} \quad \text{Eq. (11)}$$

$$D_{p,q}=\sum_{t=1}^{T} I_{t,p}\tilde{I}_{t,q} \quad \text{Eq. (12)}$$

Following this notation, the inverse of the matrix in Eq. (8) can be expressed as:

$$\left(\left[I_{t,i}\right]^T\left[I_{t,i}\right]\right)^{-1}=\frac{1}{H_{1,1}H_{2,2}-H_{1,2}^2}\begin{bmatrix}H_{2,2} & -H_{2,1}\\ -H_{1,2} & H_{1,1}\end{bmatrix} \quad \text{Eq. (13)}$$

And so the analytical expression of the solution of the axle weights for a 2-axle vehicle in a B-WIM algorithm is:

$$\begin{Bmatrix}A_1\\ A_2\end{Bmatrix}=\begin{bmatrix}\frac{\left(\tilde{A}_1D_{1,1}+\tilde{A}_2D_{1,2}\right)H_{2,2}-\left(\tilde{A}_1D_{2,1}+\tilde{A}_2D_{2,2}\right)H_{2,1}}{H_{1,1}H_{2,2}-H_{1,2}^2}\\ \frac{\left(\tilde{A}_1D_{2,1}+\tilde{A}_2D_{2,2}\right)H_{1,1}-\left(\tilde{A}_1D_{1,1}+\tilde{A}_2D_{1,2}\right)H_{1,2}}{H_{1,1}H_{2,2}-H_{1,2}^2}\end{bmatrix} \quad \text{Eq. (14)}$$

This expression provides the axle weight estimates that the current B-WIM system would provide $\{A_i\}$ based on the calibrated influence lines $\left[I_{t,i}\right]$, the current influence line $\left[\tilde{I}_{t,i}\right]$ and the actual axle loads traversing the bridge $\left\{\tilde{A}_i\right\}$. In other words, Eq. (14)

shows how changes in influence line affect the axle weight predictions for a 2-axle vehicle configuration. It is particularly interesting to explore the solution when assuming that one of the axles traversing the system is weightless. For instance, if $\tilde{A}_2 = 0$ then Eq. (14) becomes:

$$\begin{Bmatrix} A_1 \\ A_2 \end{Bmatrix} = \begin{bmatrix} \dfrac{\tilde{A}_1 D_{1,1} H_{2,2} - \tilde{A}_1 D_{2,1} H_{2,1}}{H_{1,1} H_{2,2} - H_{1,2}^2} \\ \dfrac{\tilde{A}_1 D_{2,1} H_{1,1} - \tilde{A}_1 D_{1,1} H_{1,2}}{H_{1,1} H_{2,2} - H_{1,2}^2} \end{bmatrix} \quad \text{Eq. (15)}$$

This shows that the installed B-WIM system provides an estimate for both axles, even though one of the axles traversing the system has no weight. This weightless axle has been termed here VA and including it in the calculations of a B-WIM system can provide valuable information on the state of the structure. Furthermore, it can be also shown that including the VA leads to estimates in axle weights only if there are differences in the influence lines. If there have been no changes in the bridge's influence line ($[\tilde{I}_{t,i}] = [I_{t,i}]$) then from Eq. (11) and Eq. (12) we see that $D_{p,q} = H_{p,q}$ which reduce Eq. (15) to the expression in Eq. (16). To arrive to this final expression it is relevant to note that $H_{p,q} = H_{q,p}$ due to the commutative property of the product.

$$\begin{Bmatrix} A_1 \\ A_2 \end{Bmatrix} = \begin{bmatrix} \tilde{A}_1 \\ 0 \end{bmatrix} \quad \text{Eq. (16)}$$

Eq. (16) indicates that the B-WIM correctly predicts the weight of the VA if there has been no change in influence line. Weight estimates for the VA that are different to zero indicate that there has been a change in structural behaviour. More precisely, it indicates

that the influence line obtained during calibration is different to the current influence line of the structure.

Furthermore, if the axle distance d is greater than the length of the influence line L (see Figure 2) the product of influence lines of different axles is zero. Thus when $d \geq L$ then $H_{p,q} = D_{p,q} = 0$ for $p \neq q$. In this case Eq. (15) becomes Eq. (16) regardless the changes in influence lines. This result sets the limits of possible axle distances to consider in any VA calculation to the range [0, L].

The derivation presented above assumed that the weightless axle was on the back of a hypothetical 1-axle vehicle, and thus its corresponding axle weight estimate will be termed VA_B. But similar conclusions can be obtained assuming that only the front axle of the hypothetical vehicle is weightless. In this case the axle weight predicted by the B-WIM system for the front axle is accordingly called here VA_F. The concept of VA_B has been shown in Figure 1 where the d_{VA} is the distance between both axles. For convenience, negative values of d_{VA} indicate that the virtual axle is located on the back of the vehicle, whereas positive values imply that it corresponds to the front location or VA_F. The installed B-WIM system in Figure 1, which may have several sensors, estimates weights for both axles. The system provides an answer for the weightless axle only if a change in influence line has occurred.

The proposed idea is able to identify changes in shape of the influence line only, i.e., when the influence line changes only in magnitude the addition of the VA does not provide any indication of this change. This can be shown assuming that the change in influence line is proportional to a certain value C. Thus, $D_{p,q} = C \cdot H_{p,q}$ which

substituted into Eq. (15) leads to the same results as in the no damage scenario, i.e. Eq. (16). Therefore, the applicability of the VA idea is limited to situations where a change in shape of the influence line has occurred. This is the case when local damage occurs in statically indeterminate structures, like for instance, single spans bridges with rigid or semi-rigid supports, portal frames and multiple span continuous bridges. Also the method might be used to assess secondary structural elements that are statically indeterminate in any bridge typology.

For simplification purposes, the general formulation presented in this section has been derived for the particular case of a hypothetical 2-axle vehicle including one VA. However, it is possible to extend the expressions to allow for any number of axles, being the VA concept still applicable. In the sections that follow, the VA will be part of a hypothetical 3-axle vehicle.

3. Model Description

To validate the proposed idea a numerical model of a 2-axle vehicle travelling over irregular profile while traversing a beam has been used. This model is used to generate the strain signals that the B-WIM algorithm uses to determine the weights of the passing vehicle. A brief description of the model is given in this section together with the numerical values used.

The bridge has been modelled as a fixed-fixed beam in a finite element formulation using 20 elements. Numerical values for each of the considered spans are provided in Table 1. The range of Table 1 is limited to short spans given that it is the scenario where

B-WIM systems work best, i.e., weighing single vehicle events at a time. Longer spans introduce difficulties regarding the accurate location of the axles of the vehicle on the bridge (i.e., to relate them to the influence line), the higher dynamic vibrations at a lower frequency (i.e., more difficult to filter out safely while preserving the static component of the response) and the ill-conditioned nature of estimating weights for many vehicles and axles with only a few measurement locations. For all of the spans under investigation, the same Young's modulus ($3.5\ 10^{10}$ N/m^2) and damping of 3% was considered. Figure 3 shows a sketch of the beam model, element numbering and location of sensors of the B-WIM system. The calculated strains signals are corrupted with white Gaussian noise with a Signal to Noise Ratio (SNR) of 20, unless a different value is specified explicitly in the text.

Table 1: Properties of undamaged beams

Span (m)	Mass per unit length (kg/m)	Second moment of area (m^2)	Fundamental frequency (Hz)
9	16875	0.1139	21.37
11	20625	0.2080	17.48
13	24375	0.3433	14.79
15	28125	0.5273	12.82
17	31875	0.7677	11.31
19	35625	1.0717	10.12
21	39375	1.4470	9.16

Only local structural damage was considered in the numerical simulation to validate the proposed VA idea. Local damage is modelled as a reduction in stiffness of one particular element, which corresponds to a damage length of 5% (1/20) of the bridge's span. In particular, Figure 3 highlights element 9 to indicate that this element has been damaged. By default this is the damage case considered in the subsequent numerical studies, unless a different damage scenario is specified explicitly in the text.

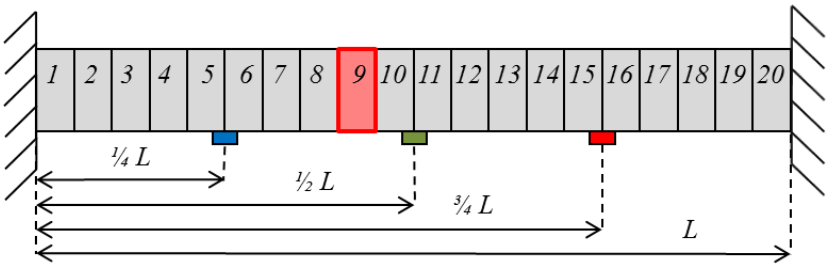

Figure 3: Sketch of FEM of beam and B-WIM sensor locations. The damaged element 9 near mid-span is highlighted.

The vehicle model that traverses the bridge is a 4-DOF system as illustrated in Figure 4. The main body and tyre masses are connected to each other and to the road profile by spring and dashpot systems. Similar models have been widely used in related literature. This simple model correctly predicts the dynamic behaviour of 2-axle vehicles taking into account the main body frequencies (bounce and pitch) as well as the frequency associated to the tyre and suspension systems. Table 2 lists the statistical variability of the vehicle properties considered, which will be used in Monte Carlo simulations in subsequent section. This vehicle model is simulated running over randomly generated road profiles according to the ISO specification [9]. Additional profile of 100 m length is added before the vehicle arrives on the bridge in order to allow for the system to reach dynamic equilibrium.

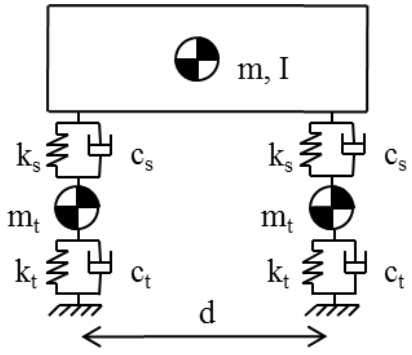

Figure 4: Sketch of vehicle model

Table 2: Variability of vehicle model properties

Property	Name	Unit	Average	Standard deviation	Minimum	Maximum
Body mass	m	kg	$10 \cdot 10^3$	$3 \cdot 10^3$	$5 \cdot 10^3$	$20 \cdot 10^3$
Body Moment of Inertia	I	kg·m^2	$100 \cdot 10^3$	$20 \cdot 10^3$	$80 \cdot 10^3$	$200 \cdot 10^3$
Suspension Stiffness	k_s	N/m	$1 \cdot 10^6$	$300 \cdot 10^3$	$500 \cdot 10^3$	$2 \cdot 10^6$
Suspension damping	c_s	N·s/m	$10 \cdot 10^3$	$3 \cdot 10^3$	$5 \cdot 10^3$	$20 \cdot 10^3$
Tyre mass	m_t	kg	$1 \cdot 10^3$	$0.5 \cdot 10^3$	$0.5 \cdot 10^3$	$2 \cdot 10^3$
Tyre stiffness	k_t	N/m	$1 \cdot 10^6$	$300 \cdot 10^3$	$500 \cdot 10^3$	$2 \cdot 10^6$
Tyre damping	c_t	N·s/m	$10 \cdot 10^3$	$3 \cdot 10^3$	$5 \cdot 10^3$	$20 \cdot 10^3$
Axle distance	d	m	5	1	3	7
Velocity	v	km/h	80	20	50	120

The models presented above for the vehicle and the bridge are both linear. To solve the coupled equations of motion between both systems, an iterative procedure, which is common in vehicle-infrastructure interaction problems [10], is applied as follows. The iterative calculation process obtains first the vehicle response due to the track profile. The time varying contact forces are then applied to the infrastructure that results in a new track deformation. The track profile is updated and a new iteration is started. This process is repeated until the difference between two consecutive solutions is below a predefined tolerance value. It is important to note that the model solution considers the assumption that all the vehicle wheels remain in contact with the track throughout the simulation. Further details on the particularities of the models, the iterative solution and vehicle properties can be found in [11].

4. Numerical examples

This section presents numerical examples that clearly show the new concept of Virtual Axle derived in Section 2. The results obtained by the VA analysis can be summarized with a single indicator, which is also defined here.

4.1 Ideal case without dynamics

First, it is convenient to show the result of the VA analysis for an ideal situation. This example considers the case of a 2-axle vehicle traversing a bridge where the noise and the dynamic effects have been neglected. In other words, only the static contribution of the moving vehicle is used to generate the clean strain signals, disregarding the contribution of the road profile, vehicle motions, its interaction with the structure and bridge dynamics. The vehicle that traverses the bridge has 2 axles of equal weights *A* and the additional Virtual axle is located at a distance d_{VA} in front of vehicle. The B-WIM system consists of three strain gauges located at [¼, ½, ¾] of the bridge length as shown in Figure 5.

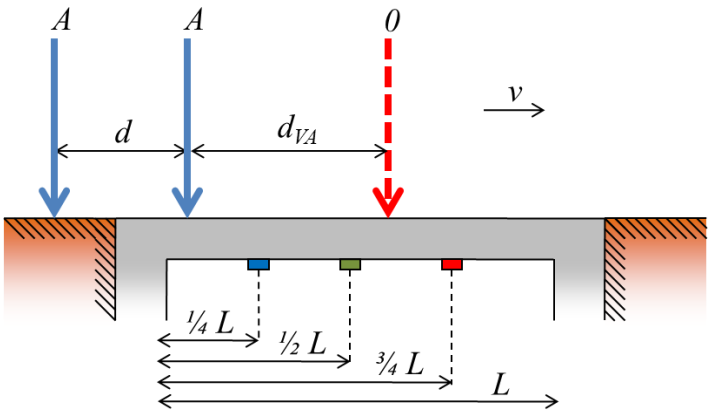

Figure 5: Sketch of 2-axle vehicle traversing a B-WIM system considering weightless axle in the front of the vehicle.

Solving the B-WIM equations for the particular situation shown in Figure 5 provides one single weight estimate for the front virtual axle (VA_F). This calculation can be repeated considering different values for d_{VA} obtaining one weight estimate for each repetition. The result of this analysis is shown in Figure 6. The values of d_{VA} that might

provide relevant results are contained within the range of [-L, L] as demonstrated in the theoretical section. Note also that negative values of d_{VA} would indicate that the weightless axle is assumed to be at a certain distance from the back of the vehicle.

The particular results presented in Figure 6 correspond to the 9 m span bridge with 30% stiffness reduction near mid-span (element 9) traversed by a vehicle with the average properties listed in Table 2. VA estimates are presented in relative magnitude as a percentage of total vehicle's gross weight (GVW). In order to have an output-only system it is necessary to obtain all the required information from the output, including the GVW. The application of the B-WIM algorithm to the real 2-axle vehicle (without any additional VA) provides estimates of the axle loads and thus the GVW of the vehicle. Then, calculations are repeated considering a hypothetical 3-axle vehicle made of the real 2-axle vehicle and a VA. Calculations are carried out placing the VA both at the front and at the rear of the real 2-axle vehicle. The results obtained for the VA shows that the presence of damage results in virtual axle predictions that change significantly with d_{VA}, where d_{VA} is the distance from VA to the closest real axle. Additionally, each sensor provides different estimates, because the modelled damage affects differently the influence lines in each location. While it is difficult to interpret the results in Figure 6 directly to assess the magnitude and location of damage it clearly shows that damage has occurred. If there is no damage the VA analysis yields zero values for any d_{VA} distance or sensor location.

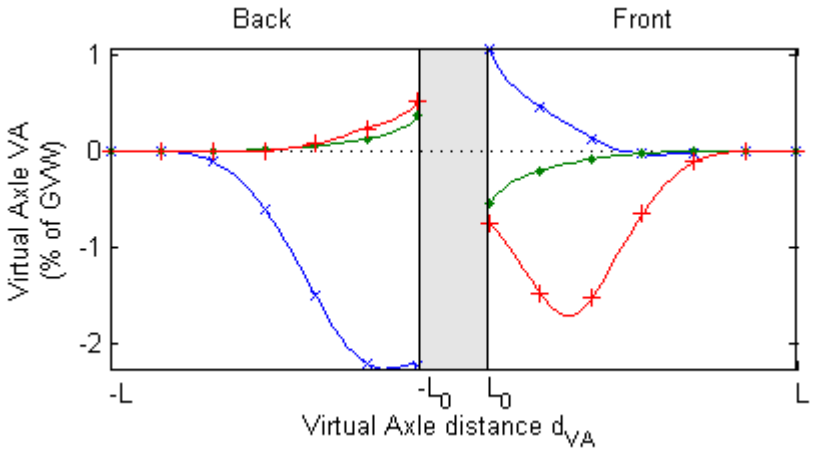

Figure 6: Virtual Axle results for B-WIM sensors at ¼ L (--x--), ½ L (--·--), and ¾ L (--+--); for 30% stiffness reduction near mid-span.

It is known that the B-WIM algorithm becomes ill conditioned for closely spaced axles. The consequences for the VA analysis are that for d_{VA} close to zero the predicted weight estimates are very sensitive to numerical perturbations in the system. Thus VA values obtained for very small d_{VA} values are not reliable. For this reason, this study does not consider d_{VA} distances (in absolute value) smaller than 10% of the bridge span. This lower boundary for the d_{VA} has been termed L_0 and is represented in Figure 6 by the shaded area in the centre.

4.2 Example including noise and dynamic effects

In any real B-WIM system the strain signals to be analysed will have noise and include dynamic effects ignored in the previous subsection. For this reason, the VA analysis is performed here on the same example as before but including now the coupled dynamic behaviour of vehicle and bridge as well as the influence of an ISO class A profile. SNR of 20 is added to all the simulated signals. Figure 7 shows the strain signals at two sensor locations for this particular example which are used to perform the VA analysis.

In these signals one can clearly appreciate the dynamic effects of the coupled system and the presence of noise.

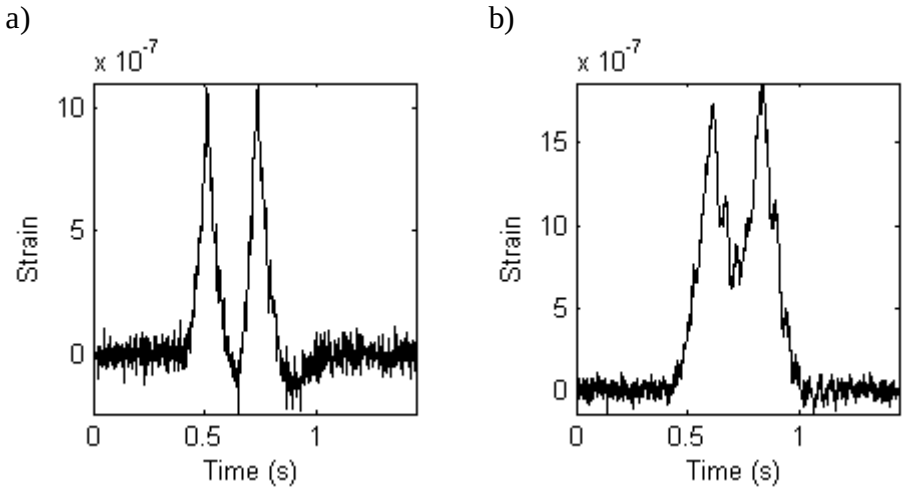

Figure 7: Strain signals of 9 m beam traversed by 2-axle vehicle measured at: a) ¼ L sensor; b) ½ L sensor

Figure 8 shows the results of two VA analyses, one for the healthy 9 m bridge (Table 1), and another including a 30% stiffness reduction near mid-span (element 9). It is relevant to note that for the no damage scenario the VA values obtained are not zero. This is due to the contribution of the dynamic effects. The strain signals are composed now of the ideal static part plus an additional dynamic contribution (Figure 7). This produces the small variations in the VA analysis results observed Figure 8.

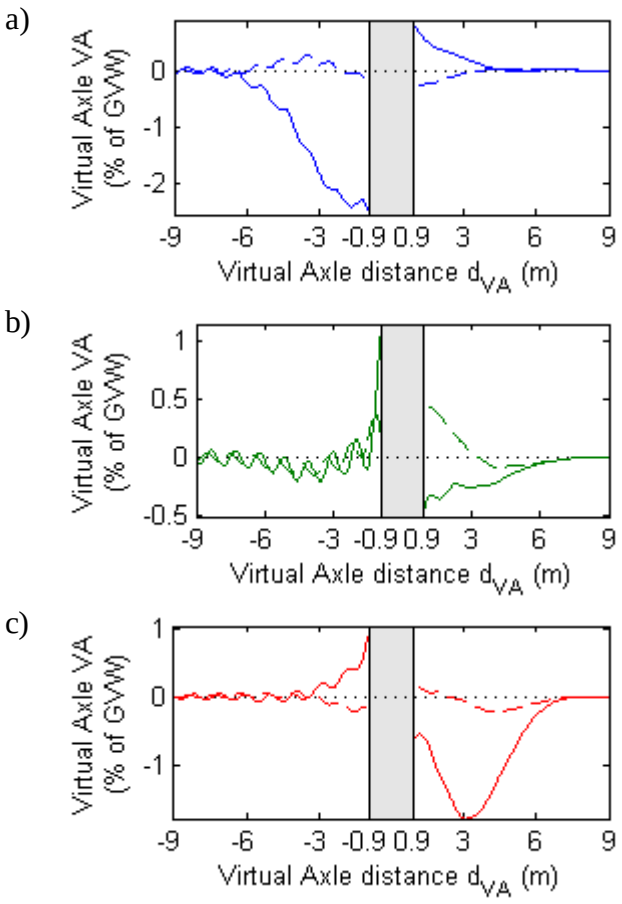

Figure 8: Virtual Axle results for healthy (dashed) and 30% stiffness reduction near mid-span (solid). For B-WIM sensor locations a) ¼ L; b) ½ L; c) ¾ L

The results are very different for each sensor and the effect of local damage is not the same in all of them. Nevertheless, the VA analysis provides clear indications that damage has occurred at least in some of the sensors. For the particular results in Figure 8 it is evident that the sensors at ¼ L and ¾ L provide the clearest indication of damage presence. The relation between the sensor location and its ability to identify damage will be discussed later in the text.

4.3 Definition of local damage indicator

The VA analysis can be performed for every vehicle that crosses a bridge instrumented with a B-WIM system. This produces several arrays of VA results for every event, one for each sensor as can be seen in Figure 8. In order to monitor changes in influence lines, it is necessary to store the results for every event over a long period of time. Managing all this data and then analysing it correctly might be a considerable task on its own. This is why there is a need of finding a value that summarizes the information obtained by the VA analysis. For practical purposes, it is suggested to use the indicator defined in Eq. (17).

$$VA^* = \frac{\int_{L_0}^{L} VA\, d(d_{VA})}{L - L_0} \qquad \text{Eq. (17)}$$

The indicator proposed in Eq. (17) represents the area of the VA results normalized by the range of d_{VA} considered. This indicator is equivalent to calculating the average value of the VA array. The authors find that the proposed indicator is a convenient way of reducing the amount of data to be analysed, while it still provides clear indications of possible changes in influence lines. Thus, for every vehicle event it is possible to calculate one value of VA^* for each sensor and each type of analysis (front and back). These values are the basis of the proposed monitoring technique, which clearly indicates even small changes in the shape of influence lines. The numerical analysis in subsequent sections shows how the proposed idea performs for a wide range of conditions.

4.4 Summary of Virtual Axle analysis

Therefore the Virtual Axle analysis can be summarized in following steps:

1) Estimate total weight of vehicle with the conventional B-WIM system.
2) Locate a weightless axle at distance d_{VA} from the vehicle.
3) Use the B-WIM algorithm considering this new axle configuration.
4) Normalize the weight estimate that corresponds to the virtual axle in terms of total vehicle weight (step 1).
5) Save d_{VA} and the normalized virtual axle result.
6) Repeat steps 2 to 5 for d_{VA} values within the range $[L_0, L]$. In this paper, a value of $L_0=L/10$ has been adopted.
7) Calculate VA^* according to Eq. (17).
8) Repeat steps 2 to 7 for negative values of d_{VA}.

5. Numerical validation

Previous sections have provided the theoretical background of the VA analysis and applied it to one specific scenario. This section aims to validate the proposed idea by means of Monte Carlo simulations. The results are compared to a common Level I damage detection technique based on monitoring changes in fundamental frequency.

5.1 Comparing performance

It is necessary to show that the proposed idea is able to detect changes in influence lines efficiently and with sufficient sensitivity. For this reason the performance of the method is compared in subsequent subsections to the changes in fundamental frequency of the structure. Given that both indicators are quantified in different units and cannot be compared directly, a simple way to compare their sensitivity to damage is by presenting the results in relative values, as presented in Eq. (18), where *k* represents the considered indicator and k_H is the corresponding indicator for the healthy structure.

$$relative\ change = \frac{k - k_H}{k_H} \qquad \text{Eq. (18)}$$

However, this common and straightforward way of comparison, has several deficiencies. First, the relative change might grow or tend to infinity for indicators that are (or tend to) zero values. This is the case of the indicator VA^* that should be close to zero if there has not been any change in influence line. Then, simply comparing changes in relative values does not take into account the variability or dispersion in the results of each of the indicators. Additionally, any indicator can be manipulated to achieve greater relative changes with damage. For instance, rather than just analysing the fundamental frequency of the structure, it might be possible to study its squared value. But in that case, the variability of the results is then also squared.

Therefore, this paper proposes the use of a dimensionless Z-score (Eq. (19)) to compare the performance of each indicator, where σ is the standard deviation for various

calculations of the considered indicator. This performance indicator correctly handles all the difficulties encountered by the relative change mentioned previously. It easily allows comparing the performance of diverse indicators, where higher Z-scores indicate greater performance. For instance, an indicator that only features very small changes with damage might still be a good indicator if its variability is also very small. On the other hand, there might be an indicator that should significantly change with damage, but due to its wide variability this effect cannot be observed. Z-score normalizes the results by its standard deviation allowing for the direct comparison of both cases.

$$Z\text{–}score = \frac{k - k_H}{\sigma} \qquad \text{Eq. (19)}$$

In the following sections the newly proposed indicator VA^* is calculated for a sample of events with random model properties. The result is a distribution of VA^* values and thus its average value and standard deviation is then used to calculate the corresponding Z-score. On the other hand, the performance of the changes in the first natural frequency is presented assuming three levels of variability expressed in terms of Coefficient of Variation (COV), namely 0.2%, 0.4% and 1%. Note that in real bridge monitoring applications the recorded natural frequencies usually have significant variations and only rarely COV below 1% have been reported [12].

5.2 Monte Carlo simulations

Monte Carlo simulations are carried out to validate the proposed VA concept and compare its performance to an alternative method based on monitoring changes in fundamental frequency. A crossing event consists of a 2-axle vehicle travelling over a

bridge with a rough profile where strain is obtained at three longitudinal locations that simulate a B-WIM installation. For every possible bridge/damage/profile configuration presented below, 200 events have been calculated and only the average and standard deviation thereof is shown in the figures. The vehicle properties have been randomly sampled following normal distribution according to Table 2, i.e., every single traffic event is different from each other. The same ISO class A profile and 9 m span bridge of Section 4 is used, except when investigating the influence of other profiles and spans.

5.2.1 Influence of degree of damage

An important aspect of the VA concept to address is its dependency with the degree of damage. Here, 31 damage magnitudes are analysed, ranging from a healthy situation (0%) to a 30% stiffness reduction near mid-span (element 9). The Monte Carlo analysis comprises 6200 events that lead to the mean and standard deviation values given in Figure 9.

Figure 9 shows results separately for front (right figures) and back (left figures) VA analysis. The shaded areas indicate that the distance to the average value is one (darker shade) and two (lighter shade) standard deviations. The boundaries of the shaded areas are obtained by finding polynomial fits in order to remove the small variations due to the randomness associated to the Monte Carlo simulation. It can be seen that VA^* change significantly with damage, particularly for the back VA for sensor at ¼L and front VA for the sensor at ¾L. Most importantly, the standard deviations are relatively small, indicating that it is possible to detect even small damage scenarios.

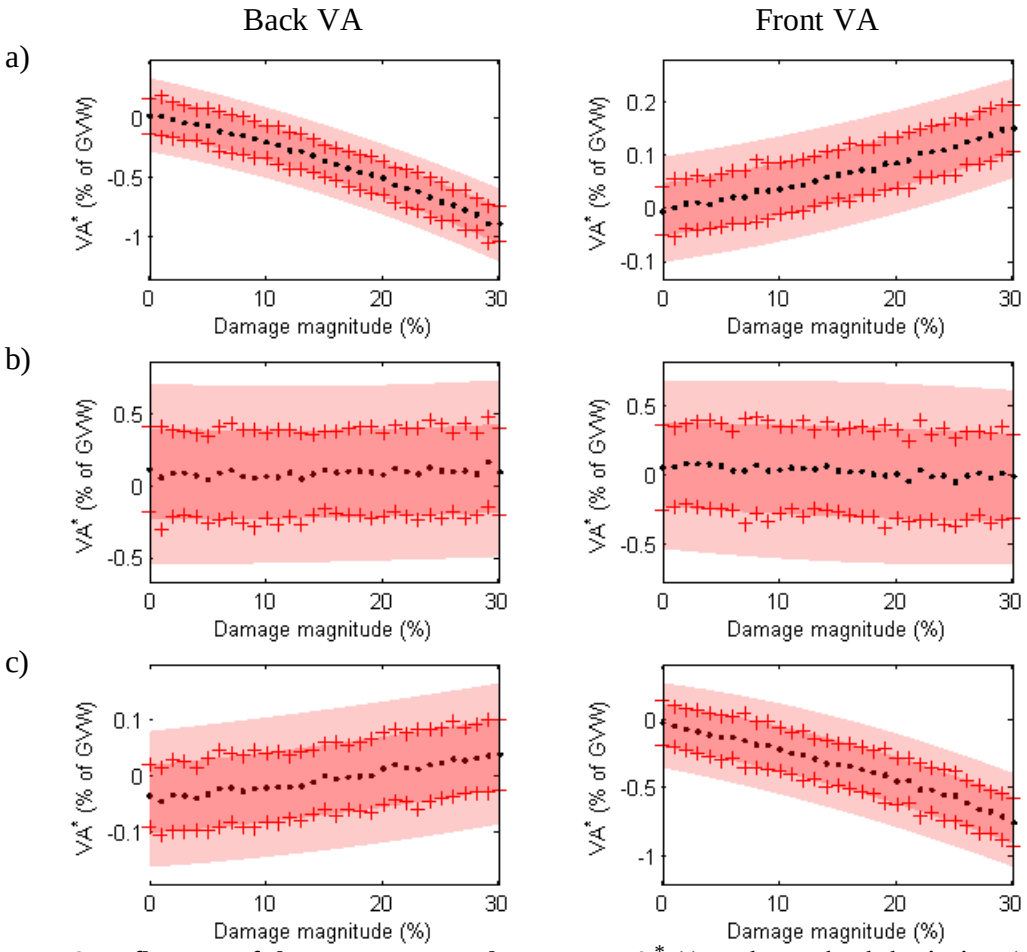

Figure 9: Influence of damage magnitude. Mean VA^* (·) and standard deviation (+) of Monte Carlo analysis. For B-WIM sensor locations a) ¼ L; b) ½ L; c) ¾ L

Furthermore, Figure 10 compares the performance of VA^* to changes in fundamental frequencies. It can be seen that performing the back VA analysis to identify damage is equivalent as being able to extract the structure's fundamental frequency with a coefficient of variation as small as 0.2%.

a) Back VA b) Front VA

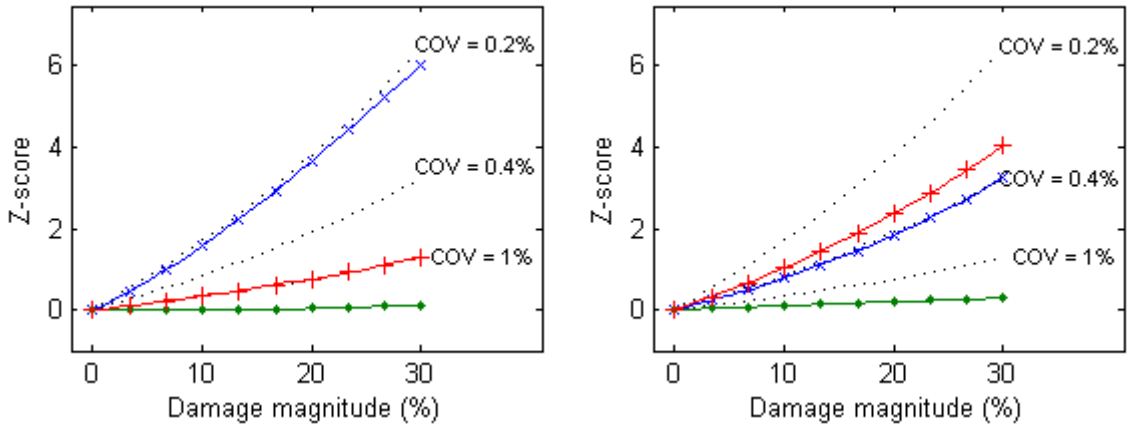

Figure 10: Performance of methods with damage magnitude, for B-WIM sensors at ¼ L (--x--), ½ L (--·--), ¾ L (--+--) and for fundamental frequency with indicated COV (· · ·).

5.2.2 Influence of damage location

Another relevant aspect for the definition of any damage detection tool is how it is affected by the location of damage. For the results in Figure 11, two levels of damage (0% and 30%) are modelled reducing the stiffness only at the element specified in the horizontal axis. The results in these figures are based on a total of 8000 events generated using Monte Carlo simulation. Figure 11 clearly shows how the actual location of the damaged element affects the mean VA^* values significantly. For a given measurement location and back (or front) VA, the variability in results appears to be relatively constant regardless the damaged element under consideration.

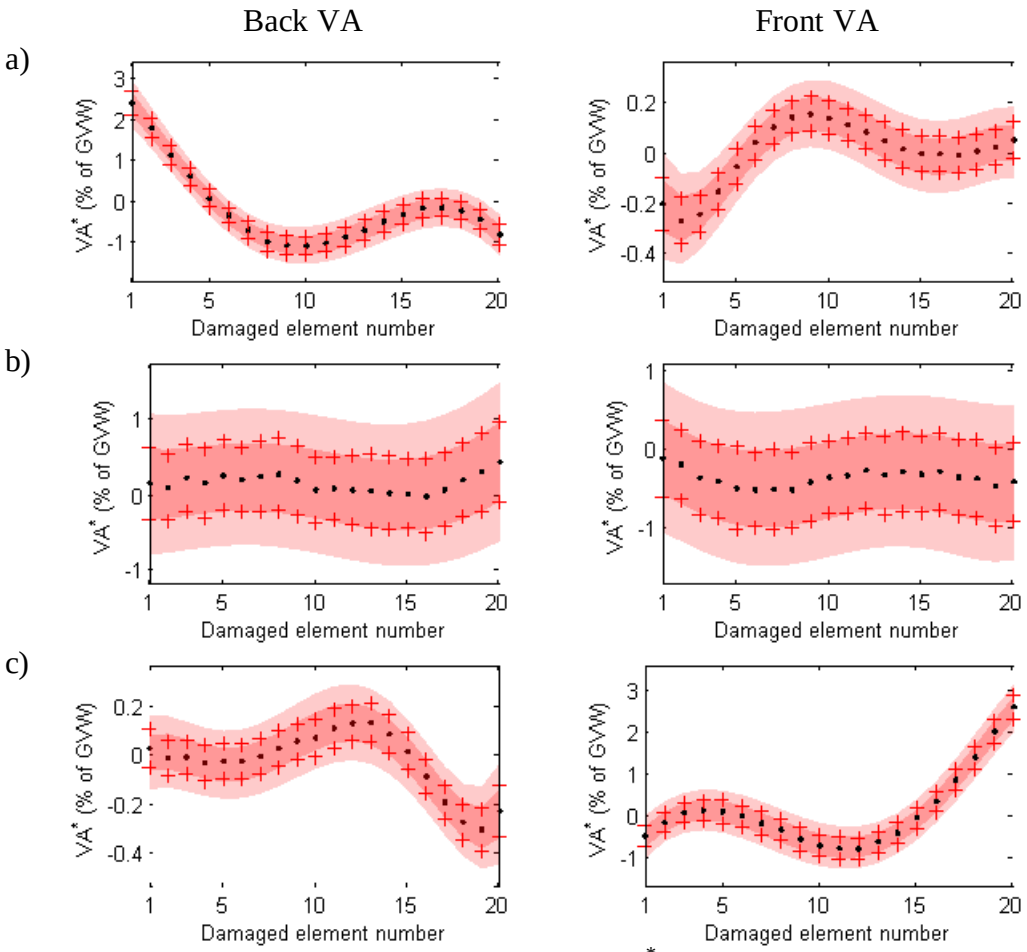

Figure 11: Influence of damage location. Mean VA^* (·) and standard deviation (+) of Monte Carlo analysis. For B-WIM sensor locations a) ¼ L; b) ½ L; c) ¾ L

The performance of VA^* is shown in Figure 12 and is compared to changes in fundamental frequency for various levels of coefficient of variation. Even though, the results vary with damage location and for each considered sensor, it can be said that there is always a sensors that provides greater or similar performances than the fundamental frequency change with a COV of 0.4%.

a) Back VA b) Front VA

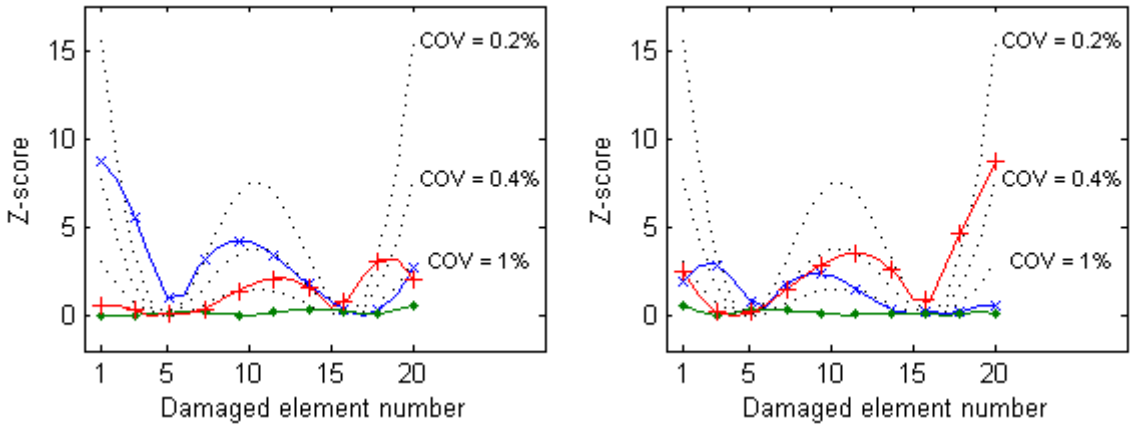

Figure 12: Performance of methods for various damage locations, for B-WIM sensors at ¼ L (--x--), ½ L (--·--), ¾ L (--+--) and for fundamental frequency with indicated COV (· · · ·).

5.2.3 Influence of noise

Real measurements on a bridge will always contain noise to some extent. For this reason a SNR of 20 was included in all the calculations of Section 5 up to this point. However noise levels can vary significantly, and be considerably large when the quality of the installed sensors is poor or the length of the transmitting cables is very long. Thus the influence of noise is investigated now studying 10 levels of SNR ranging from 5 to 50. Random vehicle properties have been used again within another Monte Carlo simulation, totalling 2000 events.

First, Figure 13a shows the influence of noise on the accuracy of the B-WIM system, without any additional VA calculations. According to the European specification [13] any WIM system can be classified with regard to the accuracy of its GVW estimates. The tolerance δ in Figure 13a indicates the width of a confidence interval in which the error remains with a specified confidence level, which for this case is 95%. The results

indicate that the B-WIM system can be classified as Class B for the range of noise levels considered. But most importantly it shows that the B-WIM is influenced only slightly by the amount of noise. This can be explained because the B-WIM algorithm essentially fits the best static response to the recorded data and high frequency components associated to noise or dynamics are removed out. The algorithm effectively works like a low-pass filter that minimizes the influence of noise. Other sources of contamination of the signal such as gradual or sudden failure of a measuring sensor will introduce a bias in the results that have not been considered. However, sensor failure could be identified from a loss of agreement between the different sensors when calculating weights using the B-WIM algorithm.

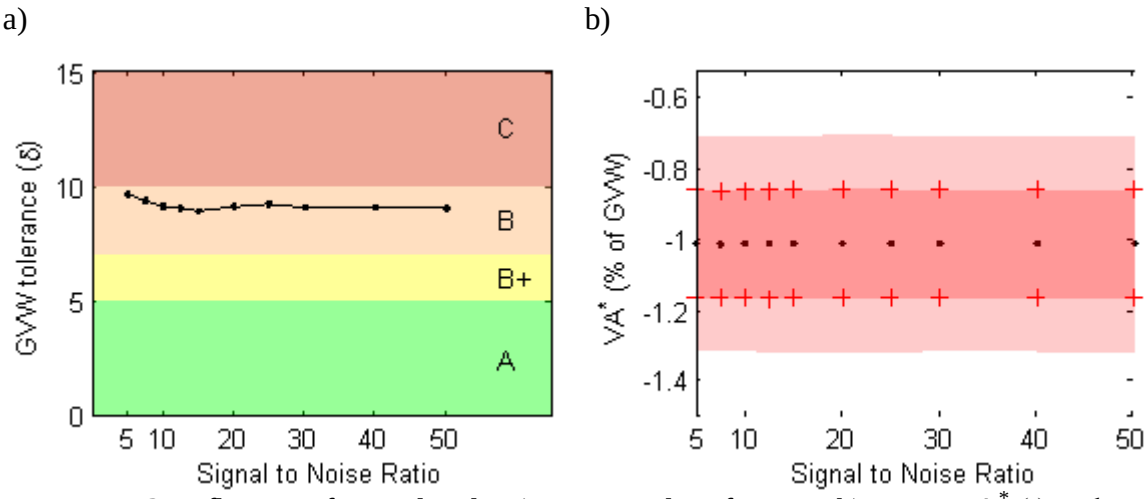

Figure 13: Influence of noise levels. a) B-WIM classification; b) Mean VA^* (·) and standard deviation (+) of Monte Carlo analysis for sensor located at ¼ L

Furthermore, Figure 13b shows the influence of noise on the mean VA^* results. Mean and standard deviations values remain almost unchanged regardless the level of noise. This can be explained, by noting that the indicator VA^* is inversely proportional to the GVW, which is estimated by the same B-WIM system. Therefore, any possible dependency of the VA result with noise is cancelled out by the noise dependency of the GVW. Therefore, the performance of VA^* indicator is not affected by the level of noise.

5.2.4 Influence of bridge span

The Virtual Axle calculations are now performed on a variety of bridge spans, defined in Table 1. This Monte Carlo simulation comprises 7 spans and 2 damage scenarios (0% and 30% stiffness reduction of element 9), totalling 2800 events. Results are shown in Figure 14 which indicates that the VA analysis might be applied to a wide range of bridges. The particular average value and standard deviations of VA^* indicator and its performance depends on the particular properties of the considered bridge.

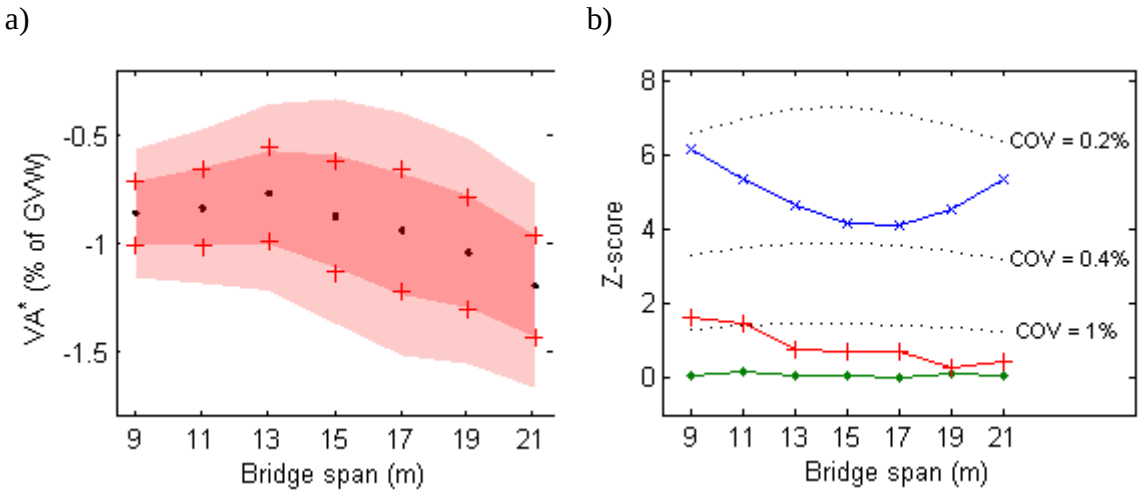

Figure 14: Bridge span influence a) Back VA* results for sensor at ¼*L*; b) Performance for B-WIM sensors at ¼ L (--x--), ½ L (--·--), ¾ L (--+--) compared to fundamental frequency performance for indicated COV (· · · ·).

5.2.5 Influence of road profile

Finally, it is worth investigating the influence of the road roughness on the performance of the algorithm. The vertical forces by the passing vehicles and the resulting bridge response depend on the particular distribution of the road irregularities on the approach and the bridge itself. Thus slightly different results are obtained for different profiles.

Rougher profiles translate generally into greater dynamics and bigger dispersion of results and in turn, more uncertainty in the VA results.

Figure 15 shows Z-score results for a sample of 30 different profiles that are classified as ISO class A, B and C according to [9]. Generally, the smoother the road profiles the higher the Z-score. For a rougher profile class, the performance of the VA method diminishes, however, it is important to note that class C correspond to 'average' profiles and only included here for completeness. Well-maintained roads and highways are expected to fall into either class A ('very good') or B ('good'). Figure 15 shows that even for class C profiles the proposed VA analysis performs better than a fundamental frequency based indicator with COV of 1%.

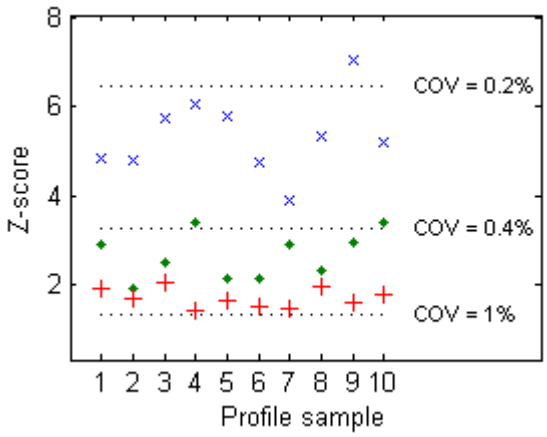

Figure 15: Influence of particular road profiles on VA performance, for Class A (x), Class B (·) and Class C (+) road profiles compared to fundamental frequency performance for indicated COV (· · · ·).

6. Discussion

The practical implementation of the VA concept for SHM can be described as follows. First, a B-WIM system should be installed and calibrated on the bridge to be monitored, i.e., following recommendations by WIM standard [13]. Then the VA analysis is

applied only to events that feature a specific population of vehicles, i.e., 2-axle heavy trucks as employed in this paper. For every event new VA* values are calculated and over time distributions of results can be characterized by their mean and standard deviation. When damage or environmental conditions produce changes in the influence lines this will be immediately reflected producing significant variations in the VA^* statistics.

Another application of the VA concept concerns automatic calibration and assessment of the accuracy of an existing BWIM system. Currently, there is no way to obtain the weight estimate errors of a B-WIM system unless the exact vehicle loads are known. The results of VA analysis are proportional to this error and might be used to indicate when a recalibration of the system is due. A problem that some B-WIM systems may face is the existence of different seasonal influence lines due influence of temperature on the support conditions, material behaviour and soil-structure interaction. Different influence lines could be defined for each season and then depending on the VA^* values the correct one could be automatically selected.

7. Conclusions

This paper has presented a novel concept for B-WIM installations, namely the 'Virtual Axle'. It is shown that it can be used as an output-only level I SHM technique for short to medium span bridges. The theoretical explanation on how the addition of a 'Virtual Axle' should be integrated into the B-WIM algorithm and why it is able to detect damage have been formulated. By means of Monte Carlo simulation the influence of various key factors on the performance of the VA method have been investigated and

compared to changes in fundamental frequency. The results have shown that VA analysis is able to detect small local damages in statically indeterminate short span structures. The location of the damage with respect to the measurement location on the bridge influences the sensitivity of the method but damage will be captured provided there are sufficient measurement locations. The method is applicable to a wide range of road conditions, while it shows very sensitivity to noise.

Acknowledgements

The work presented in this paper was performed within the Long Life Bridges project, a Marie Curie Industry-Academia Partnerships and Pathways project, funded by the European Commission 7th Framework Programme (IAPP-GA-2011-286276).

References

[1] Moses F. Weigh-In-Motion system using instrumented bridges. *ASCE* Transportation Engineering Journal 1979; 105: 233-249.

[2] OBrien EJ, Quilligan MJ, Karoumi R. Calculating an influence line from direct measurements. Bridge Engineering, Proceedings of the Institution of Civil Engineers 2006; 159: 31-34.

[3] Kalin J, Žnidarič A, Lavrič I. Practical Implementation of Nothing-on-the-Road Bridge Weigh-in-Motion System. *Slovenian National Building and Civil Engineering Institute 2006; 207: 3-10*.

[4] Liljencrantz A, Karoumi R, Olofsson P. Implementing bridge weigh-in-motion for railway traffic. Computers and Structures 2007; 85: 80–88.

[5] Cantero D, González A. Bridge damage detection using weigh-in-motion technology. ASCE Journal of Bridge Engineering (Accepted for publication).

[6] Gonzalez I, Karoumi R. BWIM Aided Damage Detection in Bridges Using Machine Learning. (Submitted for publication).

[7] OBrien EJ, Rowley CW, González A, Green MF. A regularised solution to the bridge weigh-in-motion equations. International Journal of Heavy Vehicle Systems 2009; 16: Pages 310-327.

[8] Rowley CW. Moving force identification of axle forces on bridges. University College Dublin, PhD thesis, 2007.

[9] International Organization for Standardization. Mechanical vibration – Road surface profiles - Reporting of measure data. ISO 8608:1995.

[10] Yang YB, Yau JD, Wu YS. Vehicle-Bridge interaction dynamics, with applications to high-speed railways. World Scientific; 2004.

[11] Cantero D, González A, OBrien EJ. Comparison of bridge dynamic amplification due to articulated 5-axle trucks and large cranes. Baltic Journal of Road and Bridge Engineering 2011; 6: 39-47.

[12] Hsieh KH, Halling MW, Barr PJ. Overview of vibrational structural health monitoring with representative case studies. ASCE Journal of bridge engineering 2006; 11: 707-715.

[13] European Standard. Weigh-in-Motion of Road Vehicles. Version 2010/4.